RESEARCH

Effect of baicalin on eradicating biofilms of bovine milk derived *Acinetobacter lwoffii*

Chengjun Ma[1,2,3†], Cui Mei[1,2,3†], JingJing Liu[1,2,3], Hui Li[1,2,3], Min Jiao[1,2,3], Huiming Hu[1,2,3], Yang Zhang[2,4], Jing Xiong[2,4], Yuzhang He[1,2,3], Wei Wei[1,2,3], Hongzao Yang[1,2,3*] and Hongwei Chen[1,2,3*]

Abstract

Background *Acinetobacter lwoffii* (*A.lwoffii*) is a serious zoonotic pathogen that has been identified as a cause of infections such as meningitis, bacteremia and pneumonia. In recent years, the infection rate and detection rate of *A.lwoffii* is increasing, especially in the breeding industry. Due to the presence of biofilms, it is difficult to eradicate and has become a potential super drug-resistant bacteria. Therefore, eradication of preformed biofilm is an alternative therapeutic action to control *A.lwoffii* infection. The present study aimed to clarify that baicalin could eradicate *A.lwoffii* biofilm in dairy cows, and to explore the mechanism of baicalin eradicating *A.lwoffii*.

Results The results showed that compared to the control group, the 4 MIC of baicalin significantly eradicated the preformed biofilm, and the effect was stable at this concentration, the number of viable bacteria in the biofilm was decreased by 0.67 $Log_{10}CFU/mL$. The total fluorescence intensity of biofilm bacteria decreased significantly, with a reduction rate of 67.0%. There were 833 differentially expressed genes (367 up-regulated and 466 down-regulated), whose functions mainly focused on oxidative phosphorylation, biofilm regulation system and trehalose synthesis. Molecular docking analysis predicted 11 groups of target proteins that were well combined with baicalin, and the content of trehalose decreased significantly after the biofilm of *A.lwoffii* was treated with baicalin.

Conclusions The present study evaluated the antibiofilm potential of baicalin against *A.lwoffii*. Baicalin revealed strong antibiofilm potential against *A.lwoffii*. Baicalin induced biofilm eradication may be related to oxidative phosphorylation and TCSs. Moreover, the decrease of trehalose content may be related to biofilm eradication.

Keywords Baicalin, *Acinetobacter lwoffii*, Biofilm, Eradication, Trehalose

†Chengjun Ma and Cui Mei are contributed equally to this work.

*Correspondence:
Hongzao Yang
yhz03008@swu.edu.cn
Hongwei Chen
dyxchw@swu.edu.cn
[1] College of Veterinary Medicine, Southwest University, Chongqing 402460, China
[2] National Center of Technology Innovation for Pigs, Chongqing 402460, China
[3] Present Address: Immunology Research Center, Medical Research Institute, Southwest University, Chongqing 402460, China
[4] Chongqing Academy of Animal Sciences, Chongqing 402460, China

Background

Following with the continuous development of dairy farming in China, the incidence of mastitis in dairy cows is also on the rise. Infections associated with biofilms of *Klebsiella pneumoniae* and *Acinetobacter baumannii* are the main culprits for the persistent mastitis in dairy cows [1, 2]. In recent years, the infection rate and detection rate of *A.lwoffii* have been increasing. Its resistance to penicillins and cephalosporins can reach more than 50%, showing a phenomenon of multiple drug resistance, and the resistance rate is rising rapidly [3]. Biofilm is widely recognized as the dominant mode of bacterial

Ma *et al. BMC Veterinary Research*   (2024) 20:212

Page 2 of 12

growth in nature [4]. Bacterial biofilms are surrounded by extracellular polymeric substances (EPS), which act as diffusion barriers to inhibit the deep penetration of traditional antibiotics [5]. The major components of EPS are exopolysaccharides (which are sometimes called EPSs), proteins, extracellular DNA, lipids and other biopolymers [6]. It has been extensively reported that the tolerance of biofilms to various antibiotics is 10–1000 times greater than that of planktonic cells [4, 5, 7]. The formation of bacterial biofilm is one of the important resistance mechanisms. Due to the existence of biofilms, which are not easily eradicate, and has now become a potential super drug-resistant bacteria [8]. In addition, problems such as antibiotic residues in cows and milk seriously affect human health and the vigorous development of animal husbandry. Therefore, it is of great significance to develop efficient and low-toxicity drugs to eradicate *A.lwoffii* biofilm.

Traditional Chinese medicine (TCM), which originated in ancient China, has been widely used for prevention and treatment of various diseases in China and other countries [9]. TCM and its individual components have unique advantages in the prevention and treatment of infectious diseases, including treating the symptoms and root causes, low likelihood of drug resistance, low cost, and rich action sites. Baicalin (5,6,7-trihydroxyflavone) is one of the major flavonoid monomers purified from the roots of Scutellaria baicalensis, which is listed as a Chinese herbal medicine in the Chinese Pharmacopoeia. Numerous TCM formulae containing baicalin are widely used clinically for treating fever, bronchitis and upper respiratory tract infections [10–13]. Baicalin alone or in combination with other antibacterial agents can inhibit the biofilm formation [14, 15]. However, we rarely found the effect of baicalin on the biofilm of *A.lwoffii* in the literature, especially the biofilm eradication experiment. Considering the high economic value of dairy cows and the inadvisability of using antibiotics during lactation, our team combined literature and previous research to find that baicalin can significantly eradicate the preformed biofilm of *A.lwoffii* within 24 h, with an eradication rate of up to 50%. This work intends to combine the phenotype of *A.lwoffii* preformed biofilm with RNA-seq technology to analyze its gene expression level and initially clarify its mechanism of action at the molecular level, which helped to lay a theoretical foundation for developing baicalin as a potential biofilm eradication agent.

Results

Baicalin significantly reduced the biomass and viable bacteria of biofilms in *A.lwoffii*

MIC (minimum inhibitory concentration) on *A.lwoffii* for baicalin expressed in 2048 µg/mL. The crystal violet assay represents the biomass of *A.lwoffii*. The results showed that baicalin exhibited a more significant effect on reducing the biomass of *A.lwoffii* biofilms, with a reduction rate of 41.28% at 8 MIC. We found that baicalin reduced biomass in a dose-dependent manner, while 1/2 MIC baicalin had almost no effect in *A.lwoffii* (Fig. 1A). In addition, the viability of bacteria in the biofilm was affected by baicalin. At 8 MIC, baicalin had a significant killing rate (> 90%) of bacteria in the biofilm (Fig. 1B). Considering that the higher the drug concentration, the greater the adverse reactions in vivo and in vitro studies, this experiment finally choose concentration of 4 MIC (8192 µg/mL) for subsequent experimental research.
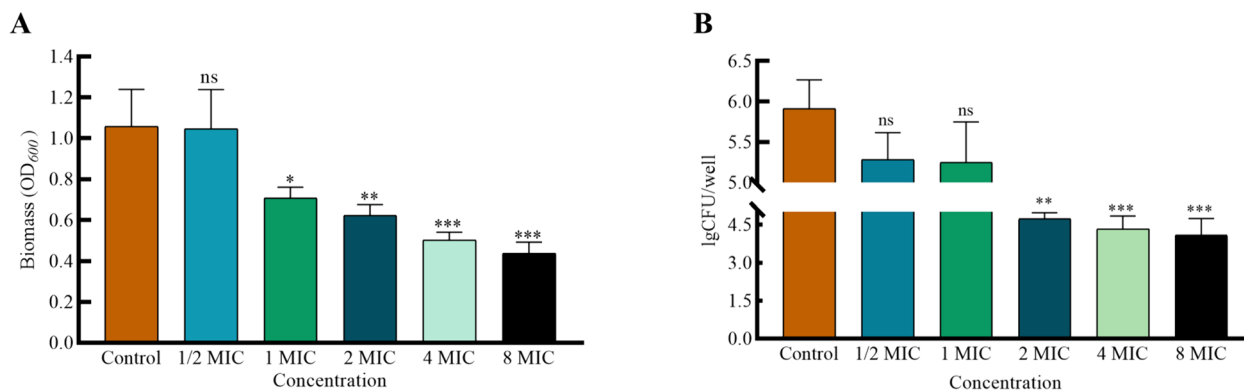

Fig. 1 Effect of baicalin on *A.Lwoffii* biofilm. *A.Lwoffii* biofilms were cultured for 24 h at 37 ℃ in 96-well plates. Post-washing, these biofilms were exposed to baicalin for 3 h. Biomass quantification was conducted using crystal violet (CV) staining (**A**) and viable bacteria of biofilm by colony counting (**B**). The significance of results was analyzed using an unpaired two-tailed t-test. Notably, * $P < 0.05$ and ** $P < 0.01$ when compared to the control group

Ma *et al. BMC Veterinary Research*   (2024) 20:212

Page 3 of 12

Baicalin eradicated biofilm of *A.lwoffii*

To corroborate the anti-biofilm activity of baicalin, confocal laser scanning microscopy (CLSM) was used to visualize the preformed biofilm after treatment with baicalin. Biofilms were grown for 24 h and then treated with baicalin for an additional 3 h, followed by staining with SYTO 9 (live) and propidium iodide (PI) (dead) bacteria. Representative orthogonal views of Z-stacks and 3D images (Fig. 2A–D) showed dead bacteria (red) and less dense structures in baicalin-treated biofilms. The results showed that baicalin markedly decreased the total fluorescence intensity of living (SYTO 9) and dead (PI) bacteria by 67% (Fig. 2E) at the concentration of 8192 μg/mL. Furthermore, the number (24.62%), area (3.89%) and volume (44.74%) of *A.Lwoffii* biofilms were decreased (Fig. 2F–H). In addition, after baicalin treatment, the ratio of fluorescence intensity per unit area to biofilm surface area decreased (F ig. 2I).

Analyzing the correlation of differential gene expression with RNA-seq technology

According to the differential gene screening criteria (qvalue < 0.05), and these differences are visualized in the volcano plot (Fig. 3A). In this plot, green dots denote genes were down-regulated (466 in total), red dots indicated up-regulated genes (367 in total), while blue dots symbolized genes with no significant changes. Subsequently, the identified genes were plotted into a Venn diagram, and the results showed that there were 2715 differentially expressed genes, including 9 unique differential genes in the control group and 34 unique differential genes in the drug group (Fig. 3B). Hierarchical clustering analysis was performed using FPKM values as expression levels (using Log10(FPKM + 1) values), and different colors represented different experimental groups. The results showed that in the control group genes clustered into one group, and genes in the drug group clustered into one group (Fig. 3C). In this work, GO software was used for analysis, and the top 30 most significantly enriched functional groups were obtained. The results showed that 20 were involved in biological processes, 7 in cellular processes, and 3 in molecular functions, mainly focusing on oxidative phosphorylation, biofilm regulation systems, and alginate synthesis (Fig. 3D). Pathway analysis of differential metabolites was performed using the Kyoto Encyclopedia of Genes and Genomes (KEGG) database, the top 20 metabolic pathways based on *p*-value were chosen for examination the alterations
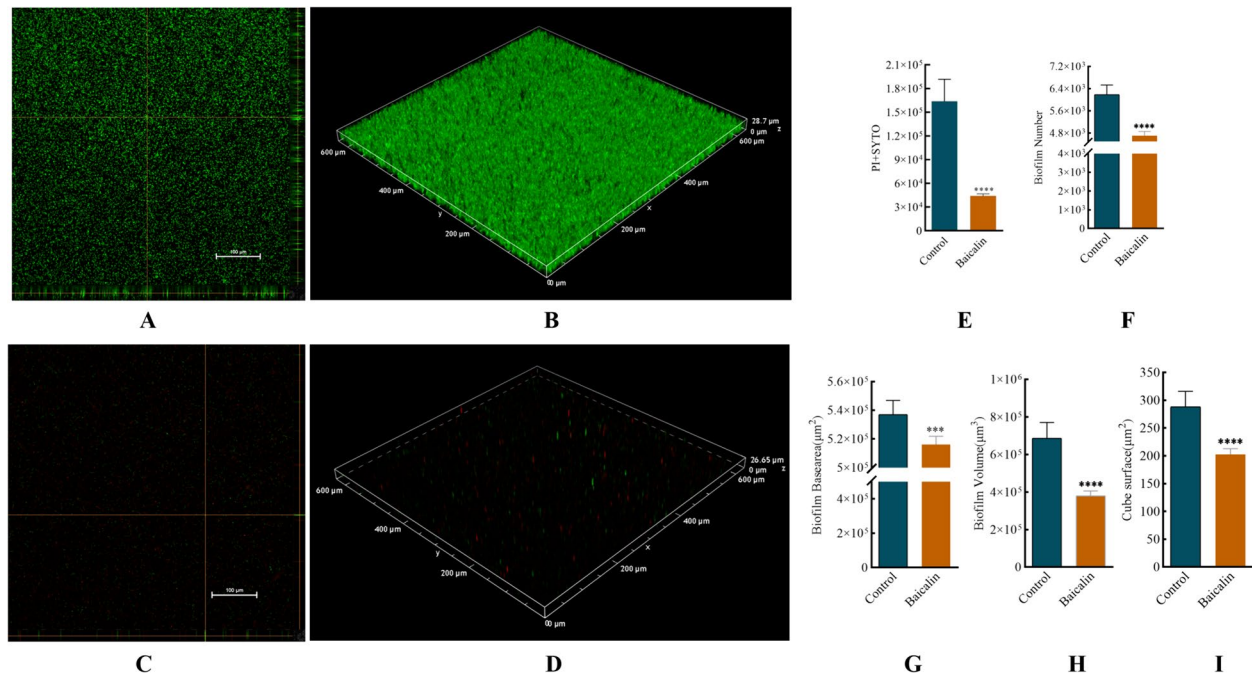

Fig. 2 CLSM analysis of baicalin treated *A.lwoffii* pre-biofilms. *A.Lwoffii* biofilm was formed for 24 h at 37 ℃ on chambered coverglass slides. After washing, biofilms were treated with baicalin for 3 h at 37 ℃ as described and subsequently stained with SYTO 9 and PI for 20 min in the dark. Images were acquired by CLSM. Using BiofilmQ software for image processing.. **A** and **B** 3D and orthogonal views biofilm representation in the objective of 20X in the control group. **C** and **D** 3D and orthogonal views biofilm representation of baicalin in the objective of 20X. **E** total fluorescence intensity of biofilms (PI + SYTO9). **F** represents the number of biofilms. **G** bottom area of biofilms. **H** represents the volume of biofilms. **I** represents the surface area of biofilms. Unpaired t-test (two-tailed) was used to measure statistical significance. * *P* < 0.05, ** *P* < 0.01 compared with the control group

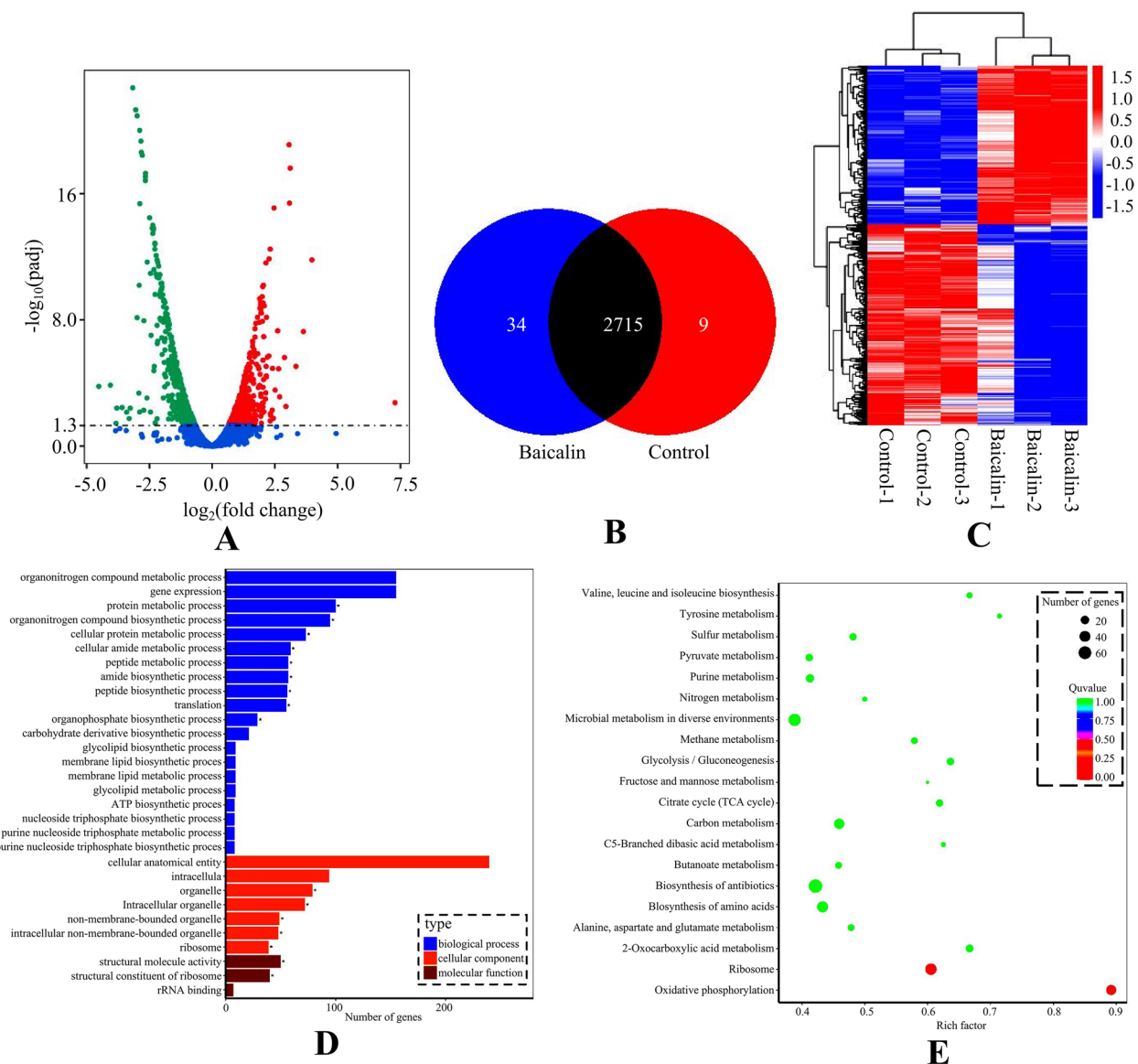Ma *et al. BMC Veterinary Research*   (2024) 20:212

Page 4 of 12

Fig. 3 Analysis of differential gene expression. The preformed biofilm was treated with 4 MIC baicalin for 3 h, and the upper culture medium in cell culture flasks was collected and centrifuged. The supernatant was taken and frozen in liquid nitrogen for storage. There were 6 samples in both the baicalin group and the control group. The samples were analyzed by LC–MS, and the data were extracted and preprocessed using Mas-terView (SCIEX). **A** Volcano plots showed the fold change of differential gene in baicalin group vs control group. The green dots represent significantly down-regulated genes (466), the red dots represent significantly up-regulated genes (367), and grey dots represent non-significantly changed differential genes. **B** Venn diagram. **C** Cluster analysis diagram of differentially expressed genes, the twenty-four hours *A.Lwoffii* pre-biofilms was treated with baicalin (4 MIC) for 3h, and the untreated biofilms was used as the control. All experiments were performed at least in triplicate, and there were 6 samples in both the baicalin group and the control group. **D** GO annotation enrichmentan analysis diagram and (**E**) KEGG enrichment analysis diagram. The *p* value is the significance of enrichment of this metabolic pathway. The ordinate is the name of the metabolic pathway, the abscissa is the rich factor. The larger the rich factor, the more metabolites enriched in the pathway. The size of the dots represents the number of differential metabolites enriched into the pathway

of total KEGG metabolic pathway (Fig. 3E). In order to sort out the relationship between differentially expressed genes and biofilms, combined with the correlation of phenotype analysis results in previous research. Classification and sorting were carried out from two-component regulatory systems, virulence factors, sugar metabolism and other regulatory pathways. The results showed that there were 26 significantly different representative genes, and the function relevance of the genes were described as follows (Table 1).

Ma *et al. BMC Veterinary Research*　　　(2024) 20:212

Page 5 of 12

Table 1 Baicalin intervention genes related to the biofilm of *A.lwoffii*

NO	Gene ID	Gene	Product	log2 |Fold Change|	P-agjust
1	02640	*ahpC*	Alkyl hydroperoxide reductase C	7.2832	1.78×10^{-3}
2	01420	*betL_3*	HTH-type transcriptional regulator BetI	3.9768	1.61×10^{-12}
3	01069	*sodB_1*	Superoxide dismutase [Mn/Fe]	3.3389	8.92×10^{-12}
4	00418	*hmp_1*	Flavohemo protein	3.0815	4.05×10^{-16}
5	00417	*nsrR*	HTH-type transcriptional repressor NsrR	3.0652	7.95×10^{-20}
6	01421	*betB*	NAD/NADP-dependent betaine aldehyde dehydrogenase	2.881	2.43×10^{-6}
7	01773	*clpB*	Chaperone protein ClpB	2.4656	8.14×10^{-16}
8	02952	*mprA*	Response regulator MprA	2.4094	1.19×10^{-5}
9	02669	*sdpR*	Transcriptional repressor SdpR	2.3932	5.30×10^{-3}
10	00867	*rhtC_2*	Threonine efflux protein	2.3209	8.94×10^{-3}
11	02960	*blC_3*	Outer membrane lipoprotein Blc	2.2581	1.94×10^{-6}
12	00618	*ppiC*	Peptidyl-prolyl cis–trans isomerase C	2.1985	2.33×10^{-6}
13	02956	*ufaA1*	Tuberculostearic acid methyltransferase UfaA1	2.1685	6.93×10^{-6}
14	02086	*otsA*	Trehalose-6-phosphate synthase	2.1662	4.15×10^{-5}
15	00619	*mutM*	Formamidopyrimidine-DNA glycosylase	2.1556	3.53×10^{-5}
16	01763	*liuE*	3-hydroxy-3-isohexenylglutaryl-CoA/hydroxy-methylglutaryl-CoA lyase	2.0776	1.29×10^{-9}
17	02555	*htpG*	Chaperone protein HtpG	2.0441	6.41×10^{-11}
18	01452	*fumC*	Fumarate hydratase class II	2.0231	1.87×10^{-4}
19	02085	*otsB*	Trehalose-6-phosphate phosphatase	2.0008	1.96×10^{-3}
20	00105	*tnsA*	Transposon Tn7 transposition protein TnsA	1.9409	3.70×10^{-9}
21	00764	*lolA*	Outer-membrane lipoprotein carrier protein	1.9001	1.81×10^{-9}
22	02286	*rcsC_3*	Sensor histidine kinase RcsC	1.7063	3.62×10^{-9}
23	00450	*mymA*	Putative FAD-containing monooxygenase MymA	1.5207	1.27×10^{-6}
24	02799	*yidC*	Membrane protein insertase YidC	-2.0796	1.37×10^{-11}
25	02566	*rplJ*	50S ribosomal protein L10	-2.3429	2.05×10^{-14}
26	02565	*rplL*	50S ribosomal protein L7/L12	-2.3674	1.02×10^{-14}

qRT-PCR is used to detect the transcription level of differential genes

To verify the accuracy of RNA-Seq results, we selected the genes in Table 3 that were most relevant to this study, and used qRT-PCR to detect the transcription level of

differential genes. The results showed that there were 3 significantly down-regulated genes (*yidC,rpiJ, liuE*) and 6 significantly up-regulated genes (*otsA, betB, mprA, rcsC-3, otsB, ahpC*) (Fig. 4). Among them, *ahpC* had the highest fold increase, which was consistent with the highest

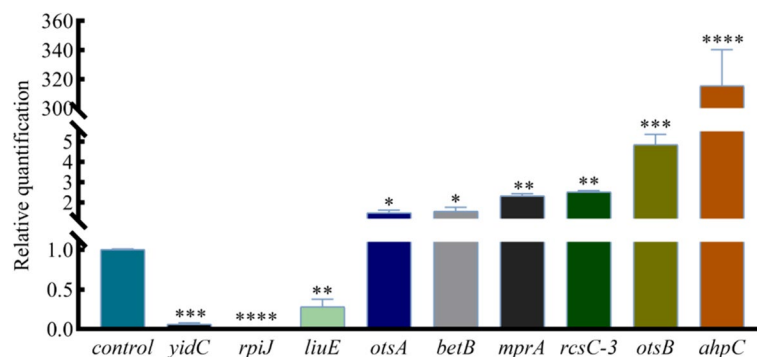**Fig. 4** Fluorescence quantitative PCR results of differential genes. Effects of 4 MIC baicalin on the regulated genes *ahpC, otsB, rcsC-3, mpaA, betB, otsA, liuE, rpiJ* and *yidC* in *A.Lwoffii* biofilms

Ma *et al. BMC Veterinary Research*   (2024) 20:212

Page 6 of 12

fold increase in transcriptome expression level. In summary, the trends of 8 genes were consistent with the transcriptome results, and the inconsistent gene was *liuE*. This indicates that the data generated by RNA-seq can be used to further study the expression of specific genes.

Molecular docking of these proteins with active ingredient
Autodock software was used to dock the active ingredient (baicalin) with 26 proteins related to the *A.lwoffii* biofilm at the molecular level. After 26 groups of target proteins and compound molecule were introduced into AutoDock Vina, the affinity value of the optimal binding postures were calculated (the results is shown in Table 2). The more stable the binding between the ligand and the receptor, the average value of 26 groups of affinity was -4.01 kcal/mol, and there are 11 groups with affinity ≤ -4.25 kcal/mol. The docking score indicates that baicalin may affect *A.Lwoffii* biofilm by regulating proteins. Figure 5 showed the docking results of baicalin with top 6 of affinity absolute value for target

Table 2 Molecular docking results of baicalin active ingredient and targets

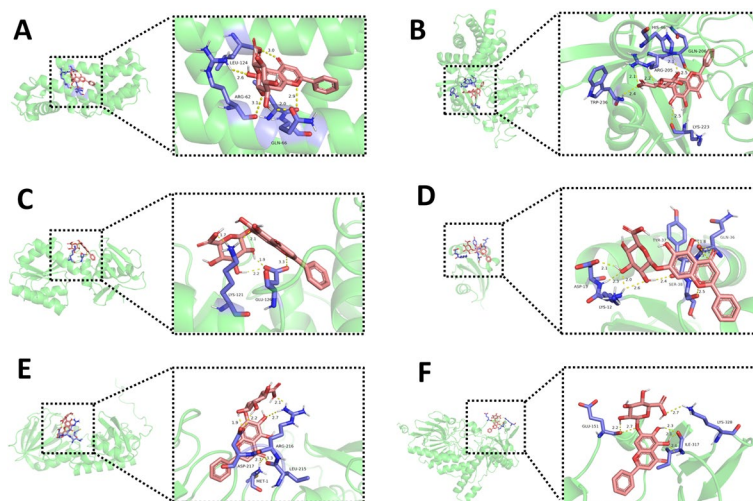| Active ingredient	Targets	Affinity/(kcal/mol)	Active ingredient	Targets	Affinity/(kcal/mol)
Baicalin	ahpC	-1.69	Baicalin	otsA	-2.95
	betL-3	-5.34		mutM	-5.67
	sodB-1	-1.64		liuE	-4.11
	hmp-1	-7.28		htpG	-2.05
	nsrR	-4.87		fumC	-3.18
	betB	-3.47		otsB	-2.97
	clpB	-2.48		tnsA	-4.36
	mprA	-6.68		lolA	-2.78
	sdpR	-4.66		rcsC-3	-3.49
	rhtC-2	-4.65		mymA	-5.02
	blC-3	-3.95		yidC	-3.25
	ppiC	-5.92		rplJ	-4.73
	ufaA1	-4.05		rplL	-2.92

Fig. 5 Three-dimensional interaction between baicalin and target proteins. AutoDockTools 1.5.7 software was applied to process proteins. PyMOL analyze the binding situation of receptor proteins and ligands in molecular docking, and it can mark hydrogen bonds. The top 6 binding force compounds were imported into PyMOL for further visualization. **A** Baicalin-betl_3, (**B**) Baicalin-hmp-1, (**C**) Baicalin-mprA, (**D**) Baicalin-ppiC, (**E**) Baicalin-mutM, (**F**). Baicalin-mymA. The yellow dotted line indicates the hydrogen bond distance or π-stacking distance, while the active ingredient is shown in red

Ma *et al. BMC Veterinary Research*   (2024) 20:212

Page 7 of 12

proteins (betL-3, hmp-1, nsrR, mprA, ppiC, mutM, mymA).

The content of trehalose significantly decreased after the biofilm of *A.lwoffii* was treated with baicalin

With trehalose content as the y-axis and the standard product concentration as the x-axis, a standard curve is drawn (Fig. 6A). Linear regression analysis gives the equation: $Y = 1.1496X + 0.0692$, $R^2 = 0.9993$. When the trehalose concentration is between 0.003125 and 0.1 mg/mL, the absorbance gradually increased with the increase of trehalose concentration. The concentration of trehalose was positively correlated with the absorbance, indicating that there was a good linear relationship between trehalose and absorbance. According to the standard curve and measurement method, the absorbance value of the sample solution collected after baicalin acted on the biofilm of *A.lwoffii* was measured. The concentration of trehalose in the test product (mg/mL) based on the trehalose standard curve was calculated. Compared with the control group, it showed that the content of trehalose in the drug group significantly decreased (Fig. 6B), indicating that the content of trehalose decreased after baicalin acted on the biofilm of *A.lwoffii*, leading to the eradication of biofilm cells.

Discussion

The genus Acinetobacter is ubiquitous in nature and is frequently found in soil, water and dry environments [16]. In recent years, the infection of *A.lwoffii* in medical clinics and livestock has been quite serious, and it is easy to cause bovine acute interstitial pneumonia, but it

has not attention has been paid to it [17]. The development speed of antibiotics has fallen far behind the evolution speed of bacterial resistance, and various resistance mechanisms have also increased the difficulty of antibiotic development [18]. One of the most significant characteristics of biofilms is lower susceptibility to antibiotic treatments and the host immune response [19, 20]. The infection rate of multi-drug resistant Gram-negative bacteria has been on the rise, and the biofilm formation is one of its important resistance mechanisms, so it is urgent to actively develop drugs for treating biofilms [21]. Baicalin has a promising antibacterial effect [22–24], MIC is 2048 μg/mL, and it has been proved that it can inhibit the formation of biofilm [10, 14, 25]. Combined with previous research, it was found that baicalin could significantly eradicate the preformed biofilm of *A.lwoffii* in the milk of cows. Therefore, combining phenotype and data analysis to study the mechanism of biofilm formation will be conducive to better clinical effects.

To the best of our knowledge, this work presented the first evidence that baicalin eradication in the *A.lwoffii* biofilm from dairy. Based on the results of biomass and biofilm bacterial assays, we concluded that baicalin can significantly reduce biomass and viable bacteria of biofilms in *A.lwoffii*. The above findings were further supported by CLSM findings. In summary, this indicates that baicalin has a significant eradicating effect on preformed biofilms of *A.lwoffii*. In addition, some studies have shown that baicalin with a certain concentration can eradicate mature biofilm of bacteria [26, 27].

RNA-seq has become the preferred technology for gene analysis, which can improve the understanding of
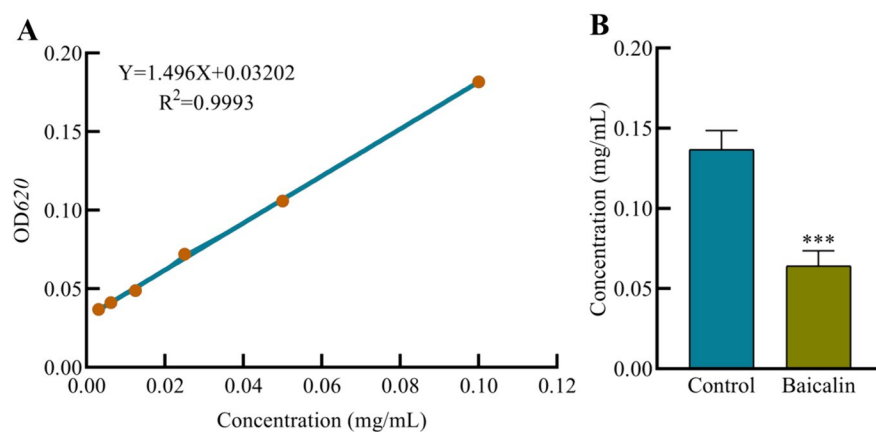

Fig. 6 Standard curve and content determination of trehalose. Sodium alginate standard product was diluted with ddH$_2$O water at a ratio, with concentrations of 0.1, 0.05, 0.025, 0.0125, 0.00625, 0.003125 mg/mL respectively. Take 0.25 mL of standard solution and 1 mL of working solution to an EP tube, water bath at 95 °C for 10 min, naturally cool to room temperature, take the solution to the colorimetric dish, measure OD_{620}nm. Calculate the concentration of ∆A standard (**A**) and using the formula obtained from the drawn standard curve to calculate X value can measure the trehalose content of each group (**B**). Unpaired t-test (two-tailed) was used to measure statistical significance. * $P < 0.05$, ** $P < 0.01$ compared with the control group

gene expression and the complexity of corresponding protein regulation. Many proteins have been proven to participate in biofilm formation, promoting or inhibiting biofilm formation by interacting with bacterial biofilm-forming proteins [27, 28]. For example, *ahpC* (alkyl hydroperoxide reductase) significantly affects the biofilm formation of *Campylobacter jejuni*, where Campylobacter oxidative stress regulator (cosR) is an important reaction regulator. ahpC is positively regulated, thereby alleviating oxidative stress of aggregates by reducing the ability of *Campylobacter jejuni* to form biofilms [29, 30]. In this study, baicalin has a good anti-oxidative stress effect, so it is speculated that baicalin may participate in the formation of *A.lwoffii* biofilm by regulating *ahpC*. *mprA* (*mycobacterium* persistence regulator) is an important regulatory factor in two-component systems (TCSs), recognizing and responding to various environmental stimuli, including environmental stimuli that induce biofilm stress, and regulating the expression of growth factors under various conditions, among which it directly regulates two key stress response factors *sigB* (sigma B, a transcriptional regulator) and *sigE* [31, 32]. Therefore, strengthening the continuous research on TCSs is crucial for understanding the interrelated regulatory network of *A.lwoffii* surviving under environmental pressure and host infection. YidC protein is a membrane-located chaperone insertase that is universally conserved in all bacteria and traditionally studied in the context of membrane protein insertion and assembly [33]; Research has found that any deficiency of *yidC* will lead to changes in the structure and physical properties of EPS matrix produced by the deformed bacteria, ultimately damaging biofilm formation, reducing its mechanical stability and promoting its eradication [34, 35]. At the same time, combined with differential gene expression analysis, it was found that Rcs phosphorylation pathway participates in the regulation of many cell surface structures in intestinal bacteria. The sensor histidine kinase RcsC autophosphorylates and transfers phosphate to the response regulator RcsB through intermediate steps. Once RcsB is phosphorylated, it regulates gene expression, thereby inhibiting the expression of biofilm-forming gene *csgD* and leading to biofilm inhibition [36, 37]. Combined with this work, it is speculated that the drug target of baicalin may be related to the above genes, providing a theoretical basis for possible drug targets for biofilm associated infections (BAI) prevention and treatment.

Molecular docking is one of most commonly used techniques in the structure-based drug design approach. This technique is generally used to understand the interaction of ligand molecules binds to the specific active site of proteins and docking score of the ligand-receptor complex was analyzed by reference ligand score. M.Abinaya

et al. found from the molecular docking analysis that the 3, 5, 7-Trihydroxyflavone can act as an anti-quorum sensing agent against *P.aeruginosa* and control the biofilm formation [38]. Vijayakumar et al. verified by Molecular docking analysis predicted the ability of hesperidin to interact with SarA and CrtM proteins involved in biofilm formation and staphyloxanthin production in MRSA [39]. To study the effect of the interactions between the 26 target proteins, which is related to the biofilm formation in *A.lwoffii*, with the baicalin was carried out the analysis of molecular docking model. In molecular docking, the lower the value of the score function, the better the affinity between the linker and the receptor [40]. As can be seen in Table 2 active ingredient showed negative binding free energy results at the active site of the protein, showing that baicalin has high affinity with the proteins. Therefore, this effectively support the baicalin can eradicate the preformed biofilm of *A.lwoffii.*

Trehalose is present in a large number of organisms and is a typical stress metabolite. It can form a unique protective film under extremely harsh conditions (such as drying, dehydration, and high osmotic pressure), protecting the structure of biomolecules from being destroyed, thereby maintaining the life characteristics of the organism [41, 42]. The genome of *Pseudomonas baumannii* encodes OtsB and OtsA. OtsA plays a key role in stress resistance and glucose metabolism, while the absence of *otsB* can affect the formation of trehalose. The genes *otsA* and *otsB* constitute an operon, and their expression is closely related to osmotic stress and stationary phase induction [43, 44]. This work found that the transcription levels of the *otsA* and *otsB* genes were upregulated by about 2 times and 4 times, respectively. It is speculated that this may be a self-protection mechanism caused by the bacterial stress response due to the intervention of baicalin in the biofilm bacteria of *A.lwoffii*. Moreover, through UV spectrophotometry, it was found that the amount of trehalose significantly decreased after the intervention of baicalin in the biofilm of *A.lwoffii*. This further indicates that trehalose may be involved in the formation of biofilms in *A.lwoffii*, and the specific mechanism needs to be further studied.

Conclusion

This study evaluated the antibiofilm potential of baicalin against *A.lwoffii*. Baicalin revealed strong antibiofilm potential against *A.lwoffii*. RT-qPCR analysis showed that the down-regulation of genes (*yidC,rpiJ*, *liuE*) involved in biofilm formation, the up-regulated genes (*otsA*, *betB*, *mprA*, *rcsC-3*, *otsB*, *ahpC*) involved in oxidative phosphorylation and TCSs in *A.lwoffii* upon baicalin treatment. Molecular docking analysis predicted the ability of baicalin to bind the active sites of target proteins in

Ma *et al. BMC Veterinary Research*   (2024) 20:212

Page 9 of 12

A.lwoffii. Moreover, the content of trehalose decreased may be related to biofilm eradication. This study suggests that baicalin may be a potential antibiofilm agent, and the mechanism of the biofilm eradication of *A.lwoffii* needs to be further studied.

Methods

Bacterial strains,culture conditions

A.lwoffii strain was resuscitated, centrifuged at $400 \times g$ for 10 min, the culture was expanded, then the supernatant was discarded and 8 mL sterile LB broth was added to resuspension. The optical density (OD) of 600 nm was adjusted to 0.1, and then diluted 100 times as the test bacterial solution.

Biomass and biofilm bacterial assays

The biomass and viable bacteria of biofilms were assayed, as described previously with minor modifications [45]. The results demonstrated that the MIC value of *A.lwoffii* to baicalin was 2048 µg/mL. The final concentrations of baicalin were 1/2 MIC, MIC, 2 MIC, 4 MIC and 8 MIC µg/mL. Strains were cultured overnight at 37 °C in Luria Bertani (LB) broth, centrifuged, diluted to 0.1 optical density at 600 nm (*OD600*) and then diluted 100 times as the test bacterial solution. The biofilms were preformed by adding the test bacterial solution into 96-well plates and incubating at 37 °C for 24 h. Afterwards, the plates were washed three times with phosphate-buffered saline (PBS). The double dilutions ranging from 8 MIC to 1/2 MIC for baicalin was prepared with LB broth. Next, 100 µL of each concentration was added to the corresponding plate and incubated at 37 °C for 3 h. Briefly, the supernatant was discarded, and the cells were washed twice with sterile PBS. Fixing with 99% methanol for 10 min, followed by air drying, staining with 0.04% crystal violet solution for 20 min, and washing with sterile PBS. Then, 33% acetic acid was used to dissolve the bound crystal violet, and absorbance was measured at OD_{600} nm. To count the number of bacteria in the biofilm, 100 µL Triton X-100 was added to each well to disrupt the biofilm, followed by tenfold dilution and spreading on TSA plates, and the colonies were counted after 12 h at 37 °C.

Confocal laser scanning microscopy (CLSM)

The morphological features of biofilms were observed by CLSM as described previously with some modifications [46]. In this experiment, 100 µL of the undiluted test bacterial solution (*OD600*=0.1) was added to an 8-well chambered cover glass (1.5 Borosilicate glass, Lab-Tek II chambered coverglass). After incubation for 24 h at 37 °C, the biofilm was treated with baicalin at 37 °C for 3 h. Then, the biofilm was washed with 0.9% (wt/vol) NaCl and stained for 20 min in the dark at room temperature

using a FilmtracerTM LIVE/DEADTM Biofilm Viability kit. After being rinsed with sterile water, the biofilm samples were imaged with a point-scanning confocal microscope, which was equipped with a Plan-Apochromat $63 \times /1.40$ oil objective lens. Signals were recorded using the green (SYTO9, excitation wavelength of 488 nm) and red (PI, excitation wavelength of 561 nm) channels. The three-dimensional (3D) image was constructed by superimposing multiple images with different Z values (z-stack). Images were acquired using ZEN (black edition) software. Four representative images were selected from each biofilm, and each experiment was repeated at least three times. The biofilm volume, area and fluorescence intensity were analyzed by BiofilmQ software [47].

RNA-seq analysis

A.lwoffii biofilms were cultured in 6-well cell culture plates for 24 h. The experimental group was treated with 4 MIC of baicalin for 3 h, simultaneously set up a broth control group. Three independent repeat samples were collected from each experimental group and sent to the company for RNA-seq sequencing. The expression levels of genes were analyzed using DESeq software. The threshold of gene expression was represented by FPKM values (0.1 or 1), and this work only analyzed genes with FPKM > 1. Differential genes were subjected to KEGG pathway and GO analysis.

Quantitative real-time PCR (RT-qPCR)

The RNA extraction and cDNA synthesis were performed using the method of Roudashti and Zhou et al. with some modifications [48, 49]. RNA was extracted from biofilms of drug groups constructed on 6-well plates. Briefly, biofilms were washed three times with pre-chilled PBS solution, and the wells were gently and thoroughly scraped, then collected in 1.5 mL centrifuge tubes. RNA extraction was performed using the Spin Column Bacteria Total RNA Purification Kit according to the manufacturer's manual. The concentration and purity of the RNA samples of per group were detected by using a Spectrophotometer (µLite, BioDrop) at 260/230 nm and 260/280 nm, respectively. Reverse transcription was performed to obtain cDNA on the basis of the manufacturer's manual at 37 °C for 15 min, 85 °C for 5 s. The cDNA samples were used for RT-qPCR detection.

RT-qPCR was used to measure the effect of 4 MIC baicalin on the expression of 8 differential genes most related to the biofilm of *A.lwoffii* using the primers listed in Table 3 (the 16 SrRNA, as the reference gene). The operationof RT-qPCR was carried out according to the instructions of the commercial kit (Takara, Prime-ScriptTM RT reagent Kit (Perfect Real Time) in a 20 µL total reaction volume. The reaction steps proceeded as

Ma *et al. BMC Veterinary Research*   (2024) 20:212

Page 10 of 12

Table 3 Gene primer sequences

Gene	Forward primer(5′ → 3′)	Reverse primer(5′ → 3′)
rcsC_3	GCGCTATTTTCAGGAACAGACC	TCTGATTGGAACTCAGCGGAAA
otsA	TTTGCCAAGCATCTGAAACAGG	GGTTACGCATACCCAGTTTTCG
otsB	GGATTGTCTGACCCACTTTCAAG	AATGAGCTTGCTGGTGAATGTG
yidC	GTTGACTCAGGGTAATGGTGAAG	CAGTACCTGCAGGCACATTAAAG
betB	ATAAATACCTGGGGCGAATCTCC	GGTCTGGGTATATTGCTGCAAAG
liuE	GGTCTGGGTATATTGCTGCAAAG	GCCCATATTCGAGAGCAGGTAA
ahpC_	GTCCAACTGAATTAGGCGATCTTG	GAGGTATCGTGCCAAGCTTTATG
rpiJ	TTCCCGTGGCGTAACTGTAG	CAGCTTCTTTTGCATCGCGT
mprA	CGGGTTATGAACTGTGTGAATGG	GCCTTTGAGTTTGTCATCCAGAG
16 SrRNA	CAGCMGCCGCGGTAATWC	CCGTCAATTCMTTTRAGTTT

follows: 40 cycles of PCR were carried out with denaturation at 95 ℃ for 30 s, annealing at 95 ℃ for 5 s and extension at 60 ℃ for 30 s. Control and experimental groups were repeated three times. The relative expression levels of each target gene were detected by $2^{-\Delta\Delta Ct}$ method.

Molecular docking

The amino acid sequences of proteins related to the biofilm of *A.lwoffii* were obtained from the protein database in NCBI (https://www.ncbi.nlm.nih.gov/). The homology model was generated and assessed using the Swiss model (https://swissmodel.expasy.org). The crystal structure of proteins was obtained from the protein database in PDB (https://www.rcsb.org/). Molecular docking was performed with the proteins as the receptor and the active ingredient as the ligand. AutoDockTools 1.5.7 software was applied to process proteins. PyMOL (https://www.pymol.org/) is an open source molecular modeling visualization software, which can analyze the binding situation of receptor proteins and ligands in molecular docking, and it can mark hydrogen bonds.The top 6 binding force compounds were imported into PyMOL for further visualization.

Assays of trehalose content

Sodium alginate standard product was diluted with ddH$_2$O water at a ratio, with concentrations of 0.1, 0.05, 0.025, 0.0125, 0.00625, 0.003125 mg/mL respectively. A volume of 0.25 mL standard solution and 1 mL working solution were added to an EP tube and boiled at 95 ℃ for 10 min. When the solution was cooled to room temperature, added the solution to the colorimetric dish and measured at OD_{620}nm. Calculate the concentration of ΔA standard (ΔA standard = A standard—A blank), with the concentration of the standard tube (self-matching concentration, mg·mL-1) as the horizontal coordinate (X-axis), and the absorbance A standard (calculated ΔA standard) as the vertical coordinate (Y-axis), draw the standard curve and perform linear regression to analyze its results. Assays of trehalose content in *A.lwoffii* biofilm by baicalin. Cultivate *A.lwoffii* biofilm for 24 h, use 4 MIC baicalin for 3 h, and set a control group, Triton lyses biofilm, centrifuge to discard supernatant; add appropriate amount of extraction solution according to the instructions, ultrasonic crushing (ultrasonic for 3 s, interval for 10 s, repeat for 30 times, 200 W), stand for 1 h, centrifuge at 8000 g for 15 min, take supernatant to EP tube, boil at 95 ℃ for 10 min, cool to room temperature, take solution to colorimetric dish, measure OD_{620}nm. Using the formula obtained from the drawn standard curve to calculate X value can measure the trehalose content of each group.

Statistical analysis

All experiments were performed in at least three independent assays. The experimental data was processed using GraphPad Prism 8.0 and Microsoft Excel software, and analyzed using Student's t-test and one-way analysis of variance. Significant differences are indicated as *($P < 0.05$), **($P < 0.01$), ***($P < 0.001$), and ****($P < 0.0001$).

Abbreviations

EPS	Extracellular polymeric substances
TCM	Traditional chinese medicine
TCSs	Two-component systems
MIC	Minimum inhibitory concentration
CLSM	Confocal laser scanning microscopy
PI	Propidium iodide
FPKM	Fragments per kilobase million
KEGG	Kyoto encyclopedia of genes and genomes
GO	Gene ontology
qRT-PCR	Quantitative real-time PCR
TCRS	Two-component regulatory systems
BAI	Biofilm associated infections
LB	Luria bertani
PBS	Phosphate-buffered saline

Supplementary Information

Authors' contributions

HWC and YZH conceived and designed the experiments. CM, CJM, HL, JJL and MJ performed the experiments. HMH, YZ, JX and YZH contributed by

Ma *et al. BMC Veterinary Research*   (2024) 20:212

Page 11 of 12

Declarations

Ethics approval and consent to participate
Not applicable.

Consent for publication
Not applicable.

Competing interests
The authors declare no competing interests.

References

1. Fu S, Wen C, Wang Z, Qiu Y, Zhang Y, Zuo J, Xu Y, Han X, Luo Z, Chen W, et al. Molecular Epidemiology and Antimicrobial Resistance of Outbreaks of Klebsiella pneumoniae Clinical Mastitis in Chinese Dairy Farms. Microbiol Spectr. 2022;10: e299722. https://doi.org/10.1128/spectrum.02997-22.
2. Avery TM, Boone RL, Lu J, Spicer SK, Guevara MA, Moore RE, Chambers SA, Manning SD, Dent L, Marshall D, et al. Analysis of Antimicrobial and Antibiofilm Activity of Human Milk Lactoferrin Compared to Bovine Lactoferrin against Multidrug Resistant and Susceptible Acinetobacter baumannii Clinical Isolates. ACS Infect Dis. 2021;7:2116–26. https://doi.org/10.1021/acsinfecdis.1c00087.
3. Xu N, Qiu C, Yang Q, Zhang Y, Wang M, Ye C, Guo M. Analysis of Phenol Biodegradation in Antibiotic and Heavy Metal Resistant Acinetobacter lwoffii NL1. Front Microbiol. 2021;12: 725755. https://doi.org/10.3389/fmicb.2021.725755.
4. Rumbaugh KP, Sauer K. Biofilm dispersion. Nat Rev Microbiol. 2020;18:571–86. https://doi.org/10.1038/s41579-020-0385-0.
5. Ju X, Chen J, Zhou M, Zhu M, Li Z, Gao S, Ou J, Xu D, Wu M, Jiang S, et al. Combating Pseudomonas aeruginosa Biofilms by a Chitosan-PEG-Peptide Conjugate via Changes in Assembled Structure. ACS Appl Mater Interfaces. 2020;12:13731–8. https://doi.org/10.1021/acsami.0c02034.
6. Zhang Y, Cheng P, Wang S, Li X, Peng L, Fang R, Xiong J, Li H, Mei C, Gao J, et al. Pseudomonas aeruginosa biofilm dispersion by the mouse antimicrobial peptide CRAMP. Vet Res. 2022;53:80. https://doi.org/10.1186/s13567-022-01097-y.
7. Wu BC, Haney EF, Akhoundsadegh N, Pletzer D, Trimble MJ, Adriaans AE, Nibbering PH, Hancock R. Human organoid biofilm model for assessing antibiofilm activity of novel agents. npj Biofilms Microbomes. 2021;7:8. https://doi.org/10.1038/s41522-020-00182-4.
8. Rakitin AL, Ermakova AY, Beletsky AV, Petrova M, Mardanov AV, Ravin NV. Genome Analysis of Acinetobacter lwoffii Strains Isolated from 15 Thousand to 1.8 Million Years Permafrost Soils Aged from Revealed Their Close Relationships with Present-Day Environmental and Clinical Isolates. Biology Basel. 2021;10:871. https://doi.org/10.3390/biology10090871.
9. Gao F, Hu Y, Fang G, Yang G, Xu Z, Dou L, Chen Z, Fan G. Recent developments in the field of the determination of constituents of TCMs in body fluids of animals and human. J Pharm Biomed Anal. 2014;87:241–60. https://doi.org/10.1016/j.jpba.2013.04.006.
10. Luo J, Dong B, Wang K, Cai S, Liu T, Cheng X, Lei D, Chen Y, Li Y, Kong J, et al. Baicalin inhibits biofilm formation, attenuates the quorum sensing-controlled virulence and enhances Pseudomonas aeruginosa clearance in a mouse peritoneal implant infection model. PLoS ONE. 2017;12: e176883. https://doi.org/10.1371/journal.pone.0176883.
11. Havsteen BH. The biochemistry and medical significance of the flavonoids. Pharmacol Ther. 2002;96:67–202. https://doi.org/10.1016/s0163-7258(02)00298-x.
12 Zhang H, Chen Q, Zhou W, Gao S, Lin H, Ye S, Xu Y, Cai J. Chinese medicine injection shuanghuanglian for treatment of acute upper respiratory tract infection: a systematic review of randomized controlled trials. Evid based Complement Altern Med. 2013;2013:987326. https://doi.org/10.1155/2013/987326.
13. Wang T, Shi G, Shao J, Wu D, Yan Y, Zhang M, Cui Y, Wang C. In vitro antifungal activity of baicalin against Candida albicans biofilms via apoptotic induction. Microb Pathog. 2015;87:21–9. https://doi.org/10.1016/j.micpath.2015.07.006.
14. Wang J, Zhu J, Meng J, Qiu T, Wang W, Wang R, Liu J. Baicalin inhibits biofilm formation by influencing primary adhesion and aggregation phases in Staphylococcus saprophyticus. Vet Microbiol. 2021;262: 109242. https://doi.org/10.1016/j.vetmic.2021.109242.
15. Han J, Luo J, Du Z, Chen Y, Liu T. Synergistic Effects of Baicalin and Levofloxacin Against Hypervirulent Klebsiella pneumoniae Biofilm In Vitro. Curr Microbiol. 2023;80:126. https://doi.org/10.1007/s00284-023-03226-y.
16. Cao S, Geng Y, Yu Z, Deng L, Gan W, Wang K, Ou Y, Chen D, Huang X, Zuo Z, et al. Acinetobacter lwoffii, an emerging pathogen for fish in Schizothorax genus in China. Transbound Emerg Dis. 2018;65:1816–22. https://doi.org/10.1111/tbed.12957.
17. Kang H, Bang JY, Mo Y, Shin JW, Bae B, Cho SH, Kim HY, Kang HR. Effect of Acinetobacter lwoffii on the modulation of macrophage activation and asthmatic inflammation. Clin Exp Allergy. 2022;52:518–29. https://doi.org/10.1111/cea.14077.
18. Darby EM, Trampari E, Siasat P, Gaya MS, Alav I, Webber MA, Blair J. Molecular mechanisms of antibiotic resistance revisited. Nat Rev Microbiol. 2023;21:280–95. https://doi.org/10.1038/s41579-022-00820-y.
19. Leoni L, Landini P. Microbiological methods for target-oriented screening of biofilm inhibitors. Methods Mol Biol. 2014;1147:175–86. https://doi.org/10.1007/978-1-4939-0467-9_12.
20 Xu D, Zhang Y, Cheng P, Wang Y, Li X, Wang Z, Yi H, Chen H. Inhibitory effect of a novel chicken-derived anti-biofilm peptide on P. aeruginosa biofilms and virulence factors. Microb Pathog. 2020;149:104514. https://doi.org/10.1016/j.micpath.2020.104514.
21. Liu YJ, Li ZH, He YT, Yuan L, Sheng GP. Antibiotic resistomes in face-mask biofilm along an urban river: Multiple drivers and co-occurrence with human opportunistic pathogens. J Hazard Mater. 2023;455: 131587. https://doi.org/10.1016/j.jhazmat.2023.131587.
22. Zhao D, Du B, Xu J, Xie Q, Lu Z, Kang Y. Baicalin promotes antibacterial defenses by modulating mitochondrial function. Biochem Biophys Res Commun. 2022;621:130–6. https://doi.org/10.1016/j.bbrc.2022.06.084.
23. Wang ZZ, Jia Y, Wang G, He H, Cao L, Shi Y, Miao M, Li XM. Dynamic covalent hydrogel of natural product baicalin with antibacterial activities. RSC Adv. 2022;12:8737–42. https://doi.org/10.1039/d1ra07553e.
24. Zhao QY, Yuan FW, Liang T, Liang XC, Luo YR, Jiang M, Qing SZ, Zhang WM. Baicalin inhibits Escherichia coli isolates in bovine mastitic milk and reduces antimicrobial resistance. J Dairy Sci. 2018;101:2415–22. https://doi.org/10.3168/jds.2017-13349.
25. Zhang P, Guo Q, Wei Z, Yang Q, Guo Z, Shen L, Duan K, Chen L. Baicalin Represses Type Three Secretion System of Pseudomonas aeruginosa through PQS System. Molecules. 2021;26:1497. https://doi.org/10.3390/molecules26061497.
26. Mao Y, Liu P, Chen H, Wang Y, Li C, Wang Q. Baicalein Inhibits the Staphylococcus aureus Biofilm and the LuxS/AI-2 System in vitro. Infect Drug Resistance. 2023;16:2861–82. https://doi.org/10.2147/IDR.S406243.
27. Sadiq FA, Flint S, Sakandar HA, He G. Molecular regulation of adhesion and biofilm formation in high and low biofilm producers of Bacillus licheniformis using RNA-Seq. Biofouling. 2019;35:143–58. https://doi.org/10.1080/08927014.2019.1575960.
28. Qin N, Tan X, Jiao Y, Liu L, Zhao W, Yang S, Jia A. RNA-Seq-based transcriptome analysis of methicillin-resistant Staphylococcus aureus biofilm

Ma *et al. BMC Veterinary Research*   (2024) 20:212

Page 12 of 12

inhibition by ursolic acid and resveratrol. Sci Rep. 2014;4:5467. https://doi.org/10.1038/srep05467.

29. Wagle BR, Upadhyay A, Upadhyaya I, Shrestha S, Arsi K, Liyanage R, Venkitanarayanan K, Donoghue DJ, Donoghue AM. Trans-Cinnamaldehyde, Eugenol and Carvacrol Reduce Campylobacter jejuni Biofilms and Modulate Expression of Select Genes and Proteins. Front Microbiol. 1837;2019:10. https://doi.org/10.3389/fmicb.2019.01837.

30. Oh E, Jeon B. Role of alkyl hydroperoxide reductase (AhpC) in the biofilm formation of Campylobacter jejuni. PLoS ONE. 2014;9: e87312. https://doi.org/10.1371/journal.pone.0087312.

31. Rao, S.D.; Datta, P.; Gennaro, M.L.; Igoshin, O.A. Chaperone-Mediated Stress Sensing in Mycobacterium tuberculosis Enables Fast Activation and Sustained Response. mSystems 2021, 6, doi:https://doi.org/10.1128/mSystems.00979-20.

32. He, H.; Hovey, R.; Kane, J.; Singh, V.; Zahrt, T.C. Correction for He et al., "MprAB Is a Stress-Responsive Two-Component System That Directly Regulates Expression of Sigma Factors SigB and SigE in Mycobacterium tuberculosis". J. Bacteriol. 2020, 202, doi:https://doi.org/10.1128/JB.00443-20.

33. Dalbey RE, Kaushik S, Kuhn A. YidC as a potential antibiotic target. Biochim Biophys Acta-Mol Cell Res. 2023;1870: 119403. https://doi.org/10.1016/j.bbamcr.2022.119403.

34. Liu, Z.; Li, L.; Wang, Q.; Sadiq, F.A.; Lee, Y.; Zhao, J.; Zhang, H.; Chen, W.; Li, H.; Lu, W. Transcriptome Analysis Reveals the Genes Involved in Bifidobacterium Longum FGSZY16M3 Biofilm Formation. Microorganisms 2021, 9, doi:https://doi.org/10.3390/microorganisms9020385.

35. Palmer, S.R.; Ren, Z.; Hwang, G.; Liu, Y.; Combs, A.; Soderstrom, B.; Lara, V.P.; Khosravi, Y.; Brady, L.J.; Koo, H. et al. Streptococcus mutans yidC1 and yidC2 Impact Cell Envelope Biogenesis, the Biofilm Matrix, and Biofilm Biophysical Properties. J. Bacteriol. 2019, 201, doi:https://doi.org/10.1128/JB.00396-18.

36. Elken EM, Tan ZN, Wang Q, Jiang XY, Wang Y, Wang YM, Ma HX. Impact of Sub-MIC Eugenol on Klebsiella pneumoniae Biofilm Formation via Upregulation of rcsB. Front Vet Sci. 2022;9: 945491. https://doi.org/10.3389/fvets.2022.945491.

37. Sharma, V.K.; Bayles, D.O.; Alt, D.P.; Looft, T.; Brunelle, B.W.; Stasko, J.A. Disruption of rcsB by a duplicated sequence in a curli-producing Escherichia coli O157:H7 results in differential gene expression in relation to biofilm formation, stress responses and metabolism. BMC Microbiol. 2017, 17, doi:https://doi.org/10.1186/s12866-017-0966-x.

38. Abinaya, M.; Gayathri, M. Inhibition of biofilm formation, quorum sensing activity and molecular docking study of isolated 3, 5, 7-Trihydroxyflavone from Alstonia scholaris leaf against P.aeruginosa. Bioorganic Chem. 2019, 87, 291–301, doi:https://doi.org/10.1016/j.bioorg.2019.03.050.

39. Vijayakumar, K.; Muhilvannan, S.; Arun Vignesh, M. Hesperidin inhibits biofilm formation, virulence and staphyloxanthin synthesis in methicillin resistant Staphylococcus aureus by targeting SarA and CrtM: an in vitro and in silico approach. World J Microbiol Biotechnol 2022, 38, doi:https://doi.org/10.1007/s11274-022-03232-5.

40. Sturlese M, Bellanda M, Moro S. NMR-Assisted Molecular Docking Methodologies. Mol. Inform. 2015;34:513–25. https://doi.org/10.1002/minf.201500012.

41. Wu J, McAuliffe O, O'Byrne CP. Trehalose transport occurs via TreB in Listeria monocytogenes and it influences biofilm development and acid resistance. Int J Food Microbiol. 2023;394: 110165. https://doi.org/10.1016/j.ijfoodmicro.2023.110165.

42. Kruse AB, Maamar R, Akakpo DL, Woelber JP, Wittmer A, Vach K, Ratka-Kruger P, Al-Ahmad A. Effects of subgingival air-polishing with trehalose powder on oral biofilm during periodontal maintenance therapy: a randomized-controlled pilot study. BMC Oral Health. 2020;20:123. https://doi.org/10.1186/s12903-020-01111-9.

43. Hubloher JJ, Zeidler S, Lamosa P, Santos H, Averhoff B, Muller V. Trehalose-6-phosphate-mediated phenotypic change in Acinetobacter baumannii. Environ Microbiol. 2020;22:5156–66. https://doi.org/10.1111/1462-2920.15148.

44. Zeidler S, Hubloher J, Schabacker K, Lamosa P, Santos H, Muller V. Trehalose, a temperature- and salt-induced solute with implications in pathobiology of Acinetobacter baumannii. Environ Microbiol. 2017;19:5088–99. https://doi.org/10.1111/1462-2920.13987.

45. Chen H, Wubbolts RW, Haagsman HP, Veldhuizen E. Inhibition and Eradication of Pseudomonas aeruginosa Biofilms by Host Defence Peptides. Sci Rep. 2018;8:10446. https://doi.org/10.1038/s41598-018-28842-8.

46. Zhang Y, He X, Cheng P, Li X, Wang S, Xiong J, Li H, Wang Z, Yi H, Du H, et al. Effects of a novel anti-biofilm peptide CRAMP combined with antibiotics on the formation of Pseudomonas aeruginosa biofilms. Microb Pathog. 2021;152: 104660. https://doi.org/10.1016/j.micpath.2020.104660.

47. Hartmann R, Jeckel H, Jelli E, Singh PK, Vaidya S, Bayer M, Rode D, Vidakovic L, Diaz-Pascual F, Fong J, et al. Quantitative image analysis of microbial communities with BiofilmQ. Nat Microbiol. 2021;6:151–6. https://doi.org/10.1038/s41564-020-00817-4.

48. Roudashti S, Zeighami H, Mirshahabi H, Bahari S, Soltani A, Haghi F. Synergistic activity of sub-inhibitory concentrations of curcumin with ceftazidime and ciprofloxacin against Pseudomonas aeruginosa quorum sensing related genes and virulence traits. World J Microbiol Biotechnol. 2017;33:50. https://doi.org/10.1007/s11274-016-2195-0.

49. Zhou JW, Chen TT, Tan XJ, Sheng JY, Jia AQ. Can the quorum sensing inhibitor resveratrol function as an aminoglycoside antibiotic accelerant against Pseudomonas aeruginosa? Int J Antimicrob Agents. 2018;52:35–41. https://doi.org/10.1016/j.ijantimicag.2018.03.002.

Publisher's Note